Synthesis of Aryl-fused Bicyclo[3.1.1]heptanes (BCHeps) and Validation as Naphthyl Bioisosteres

Aidan Kerckhoffs[1], Maud Tregear[1], Pol Hernández-Lladó[1], Massimiliano Runfola[2], Holly Shearsmith[1], Nils Frank[1], Sarah E. Squire[3], Lee Moir[3], Kirsten E. Christensen[1], Fernanda Duarte[1], Kay E. Davies[3], Angela J. Russell*[1,2]

[1]*Department of Chemistry, Chemistry Research Laboratory, University of Oxford, Mansfield Road, Oxford, OX1 3TA, UK.*
[2]*Department of Pharmacology, University of Oxford, Mansfield Road, Oxford, OX1 3QT.*
[3]*Department of Physiology, Anatomy and Genetics, University of Oxford, Sherrington Road, Oxford OX1 3PT.*

ABSTRACT: While naphthalene rings are often encountered in drugs, candidates and lead molecules, they can be susceptible to cytochrome P450-mediated metabolism in biological systems and exhibit flat, sp^2-rich structures, limiting their utility in drug-like candidates. Herein, we report the first library of derivatisable aryl-fused Bicyclo[3.1.1]heptanes (BCHeps) as bioisosteric replacements for (β-)naphthalene and other fused bicyclic aromatics. We incorporate the BCHep-based naphthyl isosteres into the AhR antagonist ezutromid and observe geometrically similar exit vectors while reducing Fsp^2, and retainment of biological activity while improving metabolic stability towards CYP metabolism, validating these motifs as 'true' bioisosteric replacements for meta-substituted arenes and 2-naphthalenes.

The naphthalene ring is a frequently encountered structural motif within lead compounds and commercially available drugs and drug candidates, including propranolol, naproxen, ezutromid and terbinafine.[1,2,3] However, naphthyl groups are susceptible to metabolic degradation, often proceeding *via* a 1,2-naphthalene oxide intermediate,[4] which is transformed into glutathione adducts[5], hydroxynaphthalene derivatives[6] or *trans*-1,2-dihydro-1,2-dihydroxy naphthyl products.[7] The diols can be further oxidized to the highly electrophilic 1,4-naphthoquinone and 1,2-naphthoquinones, which covalently bind proteins and can lead to toxic side-effects.[8] These oxidative pathways have been observed for both α-napthyl[9] and β-napthyl derivatives,[10] and usually originate through oxidation by multiple cytochrome P450 (CYP) enzymes, including subfamilies CYP1A1 and CYP1B1.[11] Furthermore, the sp^2-rich naphthyl group exhibits a "flat" structure lattice, resulting in higher melting points and poor solubility, limiting its utility as a structural motif within pharmaceuticals.[12]

Consequently, the bioisosteric replacement of naphthalene is frequently undertaken in drug discovery programmes, where typically one of the benzene rings is exchanged for an alternative functionality (**Fig. 1a**). For example, Bristol-Myers-Squibb replaced the naphthalene ring with a trifluoromethyl-containing benzene during the development of BMS-641988 for the treatment of prostate cancer.[13] Vertex's early-stage naphthyl compounds were replaced with a 1,3-ditertbutylbenzene unit **2** towards the development of the FDA-approved cystic fibrosis drug Ivacaftor.[14] Similarly, previous efforts in our group during the development of second generation utrophin modulators for the treatment of Duchenne Muscular Dystrophy (DMD) involved the replacement of a 2-napthyl group with halo-phenyl or trifluoromethyl-phenyl derivatives. These replacements resulted in similarly-active compounds.[15]

Other replacement strategies include the substitution of naphthyl rings to heterobiaryls **3-4** such as quinoline, isoquinoline,[16] phthalazine[16] indene,[17] benzimidazole[18], benzothiophene[19], indole[20], and more recently, benzazaborinine **5**.[21] Saturated analogues, such as tetrahydronaphthalenes, have also been employed, which retain the rigidity and size of the original naphthyl ring system whilst introducing more 3-dimensionality and potential increased solubility.[22]

Nonetheless, the current bioisosteric replacements for naphthyl rings lack generality and suffer from poor physicochemical properties. Fused heterocyclic ring systems (**3-5**) may have significantly different properties to the parent compound, such as lipophilicity, polar surface area, and hydrogen bonding groups, which can lead to loss of biological activity.[23] These ring systems also suffer from a high degree of planarity, often linked to poor physicochemical properties. Indeed, a higher degree of saturation (higher Fsp^3) in drug molecules has been demonstrated to increase the likelihood of clinical success, often rationalised by increased solubility or more efficient filling of 3-dimensional target space.[24] The replacement of naphthyl groups with substituted phenyl rings (**1-2**) shows poor geometric overlap with the parent structure and has limited substitution possibilities. Finally, naphthyl substitution with saturated ring counterparts **6** may dramatically impact the original exit-vectors of the aryl ring substituents and limit their application as true geometrical isosteres.

The isosteric replacement of sp^2-heavy aromatic rings with sp^3-rich small-ring cage hydrocarbon systems has emerged as a promising strategy towards improving physicochemical and pharmacokinetic properties of drug candidates.[25,26] Notably, the bicyclo[1.1.1]pentane (BCP) motif **7** represents a popular approach towards the replacement of *para*-substituted arenes, with several examples displaying improved drug-like profiles (**Fig.1b**).[26,27]

Recently, Anderson and co-workers reported the synthesis and structural analysis of bicyclo[3.1.1]heptane (BCHep) derivatives **8**, which represent the *meta*-substituted arene counterpart for BCPs. The authors validated the BCHep scaffold as a novel motif for improving the pharmacokinetic and physicochemical properties of meta-substituted drug candidates.[28] However, further investigation on the biological activity of BCHep-containing lead compounds is needed to evaluate them as true bioisosteres for the *meta*-substituted arene motif. Furthermore, we considered there could be scope to fuse the BCHep scaffold with 6-membered aromatic rings, which would represent geometrical bioisosteres for fused ring systems such as naphthalene, quinoline, isoquinoline or quinazoline (**Fig.1c**).

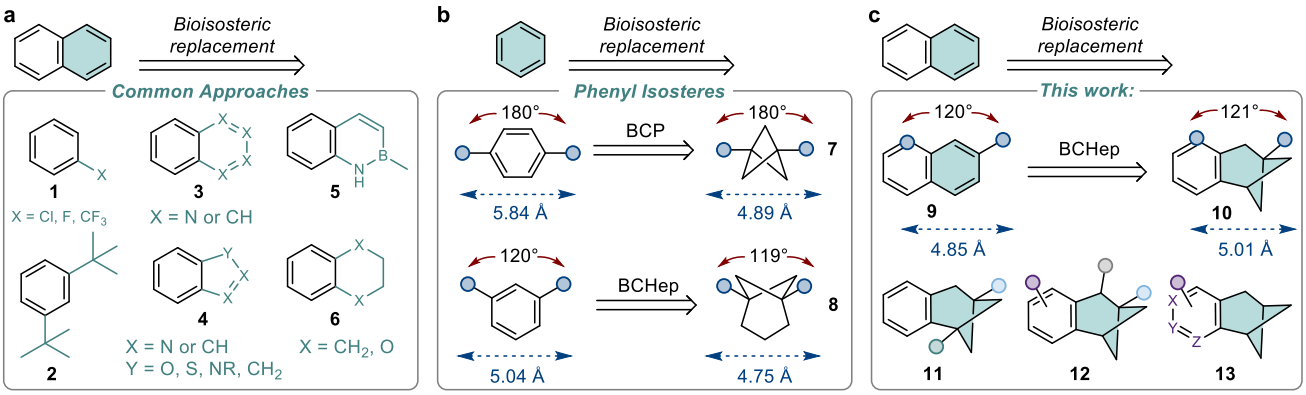

Fig.1: Common bioisosteric replacements for (a) naphthyl and (b) phenyl rings. (c) This work: development of BCHep naphthyl bioisosteres.

Herein, we report the first preparation of aryl-fused BCHep scaffolds, and establish that the geometry of the β-napthyl **9** is conserved in BCHep **10**. We extend the scope of our systems to a range of ring substitution patterns **11-12** and heterocycles **13**, providing a chemical toolbox for bioisosteric replacement of naphthalene, (iso)quinoline and quinazoline. Finally, as a proof of concept study, we bioisosterically replace the naphthyl ring of utrophin modulator ezutromid, with a range of aryl-fused BCHeps and demonstrate retainment of bioactivity whilst improving metabolic stability to CYP enzymes. This study validates that aryl-fused BCHep scaffolds can function as 'true' bioisosteric replacements for *meta*-substituted arenes and naphthalene.

RESULTS AND DISCUSSION

Compared to 'simple' meta arene isosteres **8**, we identified that BCHep derivatives of 2-naphthalene **9** benefit from three possible isostere regioisomers **10a-c** (**Fig. 2a**; colour-coded), allowing fine-tuning of molecular properties. We envisaged a general preparation of these fused ring systems *via* an intramolecular crossed [2+2] cycloaddition with a divinyl precursor **14** or **15** (**Fig. 2b**), (see ESI for full synthetic efforts). To our delight, it was possible to generate the aryl-fused BCHep framework **16** (functioning as isosteres of **17**) *via* an iridium-catalysed [2+2] photocycloaddition through visible light-induced energy transfer, adapting the methodology developed by Kwon and co-workers.[29] The authors reason that these reactions proceed *via* an excited styrene intermediate, which undergoes a formal [2+2] addition with an electron-deficient alkene, where the high selectivity arises from a stabilised benzyl radical intermediate. The iridium catalyst exhibits a suitable triplet energy for these substrates (60.1 kcal mol^{-1}) and a long-lived triplet state (τ= 2300 ns). [30]

During our studies, we prepared β-naphthyl isostere **18**, which features a convenient bridgehead ester group for further functional group transformations. Although the ^{1}H NMR spectra of the crude reaction mixtures for these reactions appeared to contain few impurities (and no observable regioisomeric bicyclo[3.2.0]heptane side product), yields were relatively modest. This prompted us to investigate the reaction progress *via* ^{1}H NMR spectroscopy.

Using dimethyl sulfone as an internal standard, the ^{1}H NMR yields ranged from 28-40% after 18 hours of reaction time. This value could not be improved upon changing the catalyst or solvent (ESI **Table S1**). When monitored over several time points, the rate of starting material consumption was significantly more rapid than product formation (**Fig.S175**). This is consistent with oligomerisation of starting material and is supported by the presence of broad peaks across the full range of the crude ^{1}H NMR spectra. It was not possible to supress oligomerisation by running the reaction under more dilute conditions (ESI **Table S2**).

Interestingly, it was possible to increase the ^{1}H NMR yield to 56% when the reaction was performed in the presence of substoichiometric amounts of pyrene for longer reaction times (ESI Table **S2**). In the presence of pyrene, we hypothesise a triplet-triplet-annihilation-upconversion (TTAU) mechanism takes place and absorption of the P-type delayed fluorescence of pyrene by the diene substrates leads to the direct formation of the singlet excited states that can undergo intramolecular cyclisation.[31] In the absence of pyrene, the excited substrates must undergo intersystem crossing from their excited triplet states to access the excited singlet state needed for ring closure to occur, thereby making oligomerisation a competing pathway.

With suitable conditions in hand, we prepared a range of aryl-fused BCHeps with varied substitution patterns to diversify the potential exit vectors of the system (and covering the three possible 2-napthyl regioisomers), whilst incorporating key functional handles for further derivatisation (**Fig. 2c**). The cycloaddition was tolerant to substitution at the benzylic position, as exemplified with alcohol **19** and ketone **20**. Fused BCHeps with doubly-substituted bridgehead positions (**21-23**) were obtained in poor yields and significantly more complicated crude mixtures, which lead to troublesome purifications. Changes to the photocatalyst or reaction solvent did not improve product yields (**ESI Fig. S175, Table S3**). Therefore, we turned our attention to less heavily substituted BCHep derivatives. In the case of bridgehead-unsubstituted substrates **24-25**, yields were higher, in line with Kwon's observations.[29] Under these conditions, the authors reported that pyridine-based substrates were not capable of undergoing [2+2] cycloadditions.[29] We speculated that this may be due to the Lewis basicity of the pyridine nitrogen. Gratifyingly, we observed that upon addition of 25 mol% diphenyl phosphoric acid to facilitate protonation of the pyridine nitrogen, [30] it was possible to generate the corresponding heterocyclic derivatives **26-28**. Finally, it was possible to prepare ether

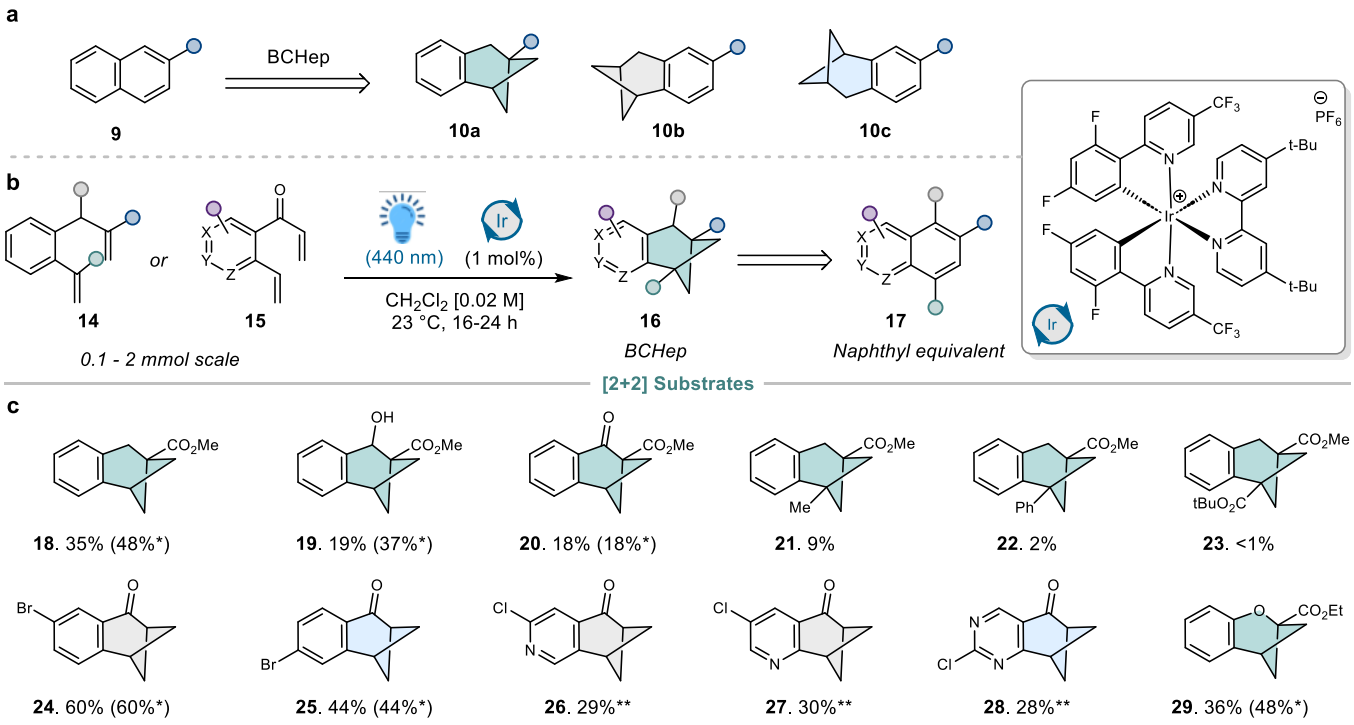

Fig.2: (a) Three possible regioisomeric bioisosteres are possible using fused BCHeps and (colour-coded by regiosomer). (b) General strategy and conditions towards generating the bicyclo[3.1.1]heptane core (c) List of [2+2] products. Isol. Yield * With 15 mol% pyrene. ** With 25 mol% diphenyl phosphoric acid

derivative **29** in similar yields to the other substrates, blocking the potentially metabolically labile benzylic CH_2 site,[32] and showcasing the versatility of the [2+2] methodology. The addition of pyrene allowed us to improve the yields for esters **18**, **19** and **29** by up to ~ 20%, whereas the triplet annihilator did not impact the yields of ketone substrates **20**, **24** and **25**.

With aryl-fused BCHeps **18-28** in hand, we explored their derivatisation to provide further building blocks (**Fig. 3**). It was possible to reduce aryl ketones **24-25** in high yields under acidic conditions to generate **29a-b**, which feature a convenient halide handle for cross-coupling. For heterocyclic derivatives **26-28**, it was necessary to reduce the ketone *via* alcohols such as **31**, followed by a deoxygenation protocol to afford saturated cross coupling partners **32-33**. Isoquinoline isostere **33** was subjected to Suzuki cross-coupling conditions with **34** to afford the highly crystalline nitroarene **35**, which was characterised *via* X-ray crystallography. The angle across the bridgehead was 119°, consistent with the original reports of the BCHep frameworks **8** by Anderson and coworkers,[28] highlighting that the bridgehead isostere geometry was not affected by the addition of a fused arene.

To complement the functionality tolerated on the (hetero)aryl ring, we sought to derivatise the bridgehead to generate a library of the underrepresented β-naphthyl isostere building blocks (**Fig.3**). Hydrolysis of **18** afforded key intermediate **36**, which was successfully amide coupled to a complex aniline towards the preparation of an ezutromid derivative (**ESI Scheme 13**). It was also possible to convert acid **36** into primary amine **37**; which is expected to display an improved safety profile relative to the commonly toxic aryl amine motif. [33] **37** could also be converted to an amide derivative (**ESI Scheme 12**).

The BCHep-derivatives are also compatible with radical chemistry at the bridgehead, with acid **36** yielding bromide **38** *via* an iridium-catalysed decarboxylative bromination,[34] and *N*-hydroxyphthalimide **39** undergoing a decarboxylative Minisci reaction to provide heterocyclic derivative **40**.[35] We also successfully prepared Weinreb amide **41** from **18**, which readily generated ketone **42**. This substrate could be brominated under mild conditions to afford bromoketone **43**, a versatile building block towards the synthesis of heterocycles.[36]

We also explored the possibility of blocking the benzylic CH_2 site by preparing mono- and difluoro derivates **44** and **46** from dithiane **45**, highlighting the potential to further suppress the metabolism of these aryl-fused BCHeps *via* CYP-mediated benzylic oxidation.[32] Finally, we generated the free acid **47** of ether **29** to elucidate the effect of the oxygen on bond angles via X-ray diffraction. We observed that the β-napthyl angle is reduced from 120° to 111°, whereas the bridgehead distances are increased to 127°. This highlights the importance of a full-carbon framework to facilitate geometrical isosterism, but allows the opportunity to modulate the angles within the naphthyl isostere framework.

We then sought to validate these scaffolds as true naphthyl isosteres by replacing the naphthalene ring of ezutromid with the BCHep motif (**Fig.4**). Ezutromid was a first-in-class utrophin modulator that was evaluated in a phase 2 clinical study for the treatment of Duchenne muscular dystrophy.[37] DMD is a disease caused by multiple different loss-of-function mutations in the gene encoding the structural muscle protein dystrophin. Ezutromid is known to function by upregulating the protein utrophin in muscle, which can compensate for the missing dystrophin in DMD patients regardless of disease mutation type.[10] Clinical studies with repeated dosing of ezutromid displayed promising 24 week data, with significantly reduced muscle fibre damage and increased levels of utrophin, providing the first evidence of target engagement and proof of mechanism. However, ezutromid failed to meet

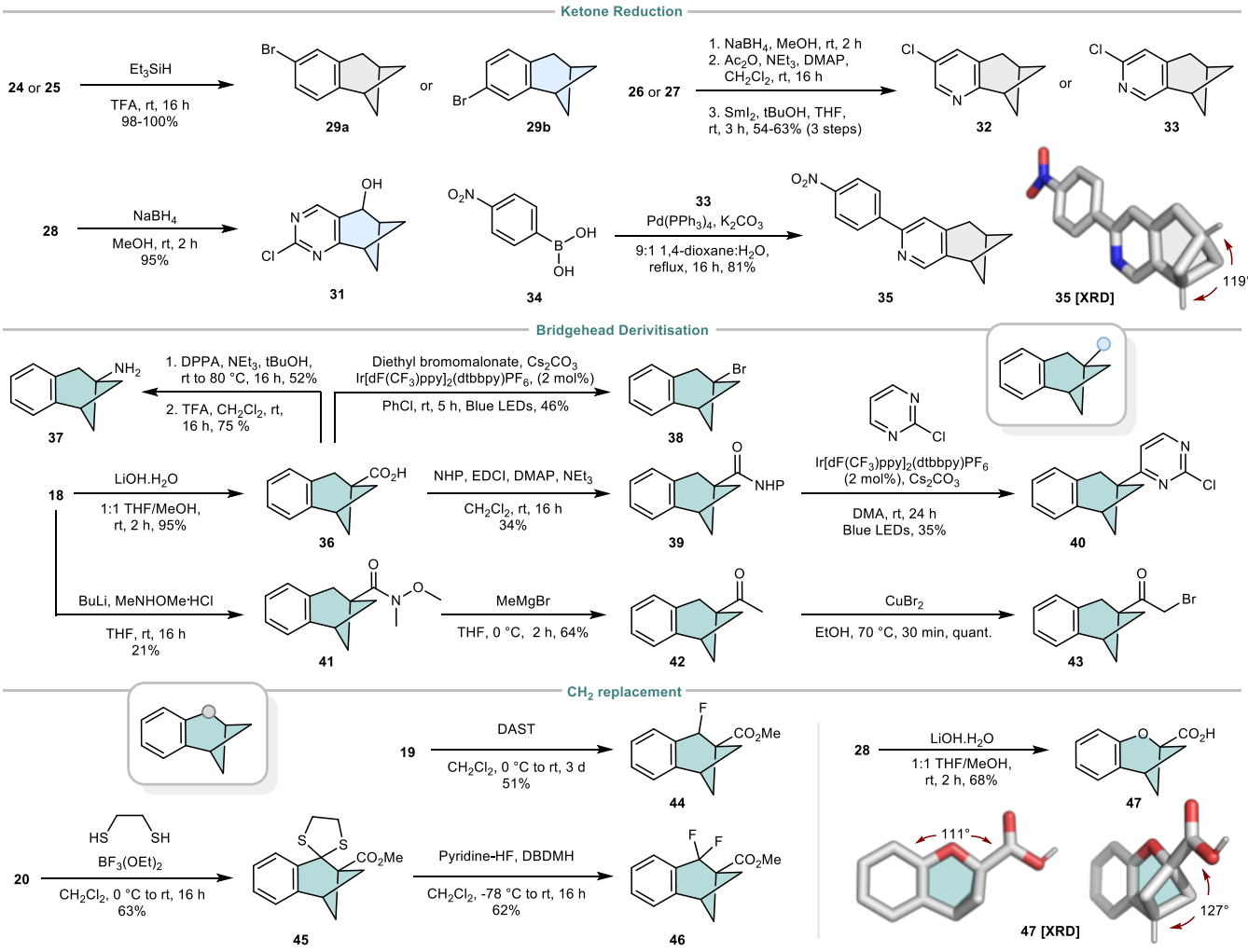

Fig.3 Derivatization of BCHep building blocks and geometrical analysis of crystalline derivatives

its primary or secondary end points after 48 weeks of treatment, and further development was discontinued.[38] Subsequent studies on ezutromid revealed that the lack of sustained therapeutic efficacy could be ascribed to the naphthalene unit which is susceptible to hepatic CYP-mediated oxidation (**Fig.4a**).[10] We previously reported that prolonged dosing of ezutromid induces a paradoxical increase in CYP1A activity resulting in a reduced exposure of the drug over time, increased production of inactive dihydrodiol metabolites **48**-**49** accounting for its reduction of efficacy over time.[10] Therefore, we envisaged the replacement of the naphthyl ring to the isosteric BCHep counterparts **50a-c** could suppress CYP1A-mediated oxidation of the naphthalene (**Fig.4b**), potentially circumventing the issue observed with ezutromid. **50a** was prepared by amide-coupling of **36** followed by condensation into the benzoxazole, whilst regioisomers **50b-c** were accessed by a C-H activation/cross coupling protocol from **29a-b** (**ESI Scheme S13**).

To compare the geometry of the BCHep motif relative to the parent compound, we prepared single crystals of regioisomers **50a-b** and ezutromid and analysed them by X-ray crystallography (**Fig. 4c-e**). To our delight, the β-naphthalene and bridgehead substituents retained the desired ~ 120 ° angle, whilst the distance between the meta substitution pattern was within 5% of the original geometry of the naphthalene isostere. Overlaying the BCHep portion of **50a-b** with the naphthyl unit of ezutromid revealed a low RMSD of ~ 0.1 (**Fig. 4f-g**), highlighting the high geometrical isosterism of these novel motifs. Overlaying the full structures still resulted in a good structural similarity across the entire drug molecule (**ESI Fig. S177**). Moreover, the calculated electrostatic potential maps for **50a** and ezutromid showed high similarity (**ESI Fig. S178-179**).

Encouraged by these results, we sought to assess the novel derivatives **50a-c** for their biological activities relative to ezutromid. To this aim, we decided to measure the activity of ezutromid and the new analogues against ezutromid's primary target, which has recently been identified as the Aryl hydrocarbon receptor (AhR).[39] This nuclear transcription factor plays a pivotal role in the metabolism of exogenous small molecules by targeting nuclear DNA to upregulate expression of some isoforms of cytochrome P450 enzymes (CYP) responsible for Phase I metabolism of drugs, such as CYP1A isoforms (**Fig. 5a**). Therefore, AhR inhibition can be monitored by measuring the relative expression of these genes, with lower *CYP1A1* mRNA levels being proportional to AhR antagonism (**Fig. 5b**).

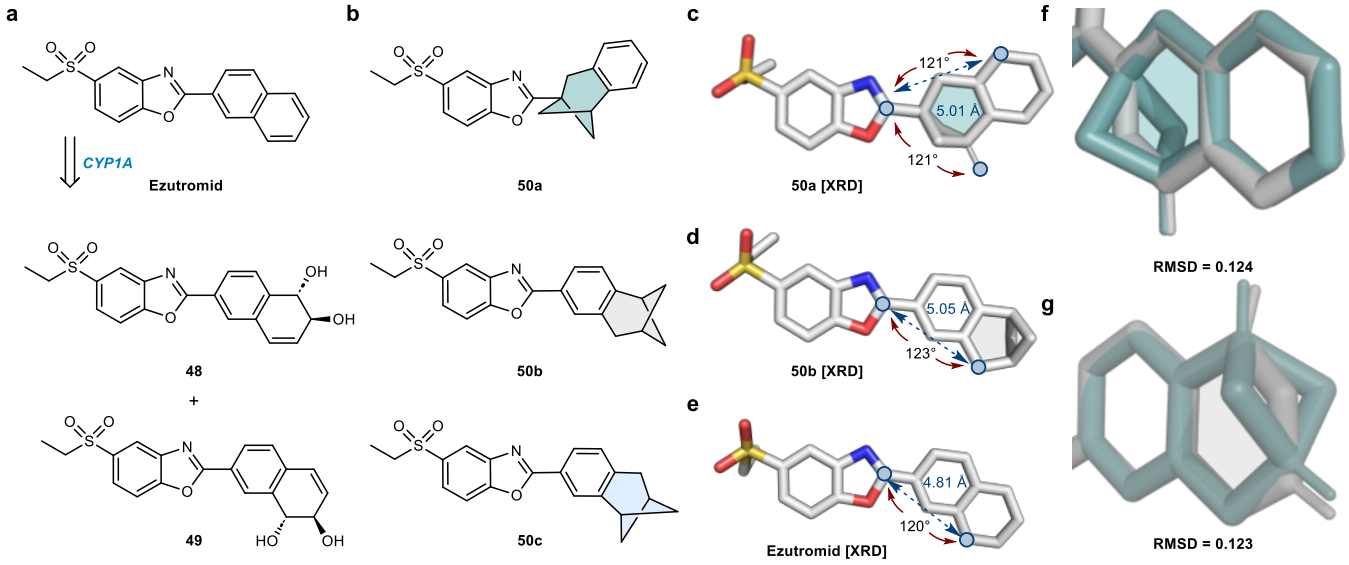

Fig.4 (a) CYP1A-mediated oxidation of Ezutromid. (b) List of BCHep-Ezutromid derivatives (c) X-ray solid-state structure of **50a**. (d) X-ray solid state structure of **50b**. (e) X-ray solid-state structure of Ezutromid (unit cell contained two 'downward' facing naphthyl conformers, where each conformer exhbits a unique sulfone conformation) (f) Stacked solid-state structures of the BCHep unit of **50a** (green) with Ezutromid (grey). (g) Stacked solid-state structures of the BCHep unit of **50b** (green) with Ezutromid (grey). RMSD values calculated using the 'pair-fit' function in Pymol and mapping the naphthyl and BCHep carbon atoms.

To determine the activity of compounds **50a-c** as AhR antagonists, we *quantified CYP1A1* mRNA levels in human liver cell line HepG2 by Real Time Quantitative Polymerase Chain Reaction (RT-qPCR) after 4 h of incubation with test compounds. Gratifyingly**,** all new analogues retained biological activity when tested at a 10 μM concentration, showing at least an 84% reduction of CYP1A1 expression (**50a**: 84.1%±2.7; **50b**: 93.9%±1.9; **50c**: 93.4%±1.5, Ezutromid: 95.1%±1.4). Interestingly, there was a significant difference

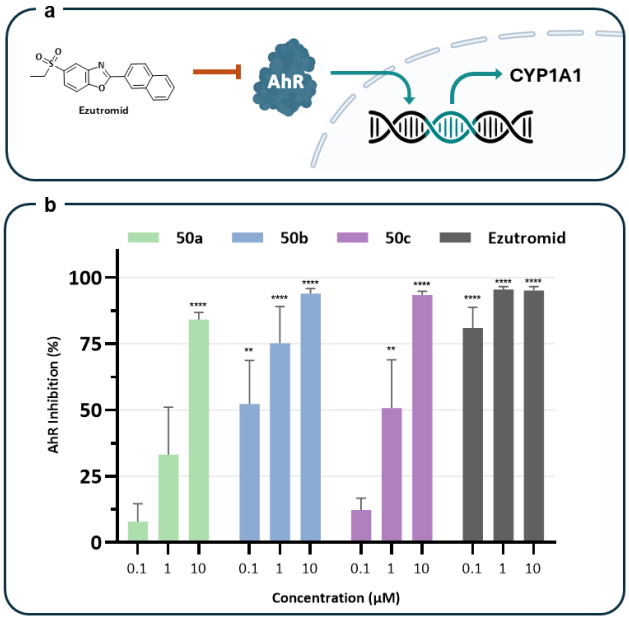

Fig.5 (a) Schematic representation of how Ezutromid antagonizes AhR preventing its translocation into the nuclei and its subsequent upregulation of CYP1A1 enzyme. Inhibition of AhR can therefore be evaluated as a decrease in CYP1A1 expression. (b) Evaluation of 50a-c as AhR antagonists compared to Ezutromid. Data have been obtained by RT-qPCR, and analysed using the $2^{-\Delta\Delta Ct}$ method. Values obtained have been normalized to control (DMSO 1%), and presented as Mean + SEM (n=4). Statistical analysis was performed using the Ordinary One-way ANOVA followed by Dunnett's multiple comparisons test against Vehicle Control: **: $p < 0.005$; ****: $p < 0.0001$ (grey).

in activity between each regioisomer of **50a-c**, perhaps indicating that there may be variations in how each compound binds to AhR. The solid-state structures reveal that the BCHep unit of the most active derivative **50b** points 'downwards' (on the oxygen side of the oxazole)**,** whereas the less active **50a** resides in a conformation where the napthyl isostere faces 'upwards' (on the nitrogen side of the oxazole); suggesting that the 'downwards' conformation is preferable for achieving higher activity. This is agreement with the highly active ezutromid, who's solid-state unit cell is a disordered structure containing two 'downwards' facing naphthyl conformers (**ESI Fig. S180**).

The computed structures of the less active **50a** and **50c** exhibit an energetic preference towards an 'upwards' BCHep conformation, whereas the most active **50b** is 'downwards', consistent with the the solid-state structures (**ESI Fig. S180**). For ezutromid, both naphthyl conformers were computationally indiscriminate in energy.

Finally, we subjected the most promising derivatives to metabolic stability studies in mouse liver microsomes, a validated model for understanding phase I metabolism of drugs (Table 1). To investigate whether the new analogues would be susceptible to CYPs metabolism, we repeated these tests in the presence of 3 μM α-naphthoflavone (ANF). ANF is a well-known inhibitor of CYP1A enzymes, which is responsible for the CYP oxidative metabolism of naphthalene ring in ezutromid.[40] Interestingly, these derivatives showed a similar or higher metabolic stability relative to ezutromid, with comparable half-lives. In particular, compound **50a** showed a ~2-fold increase in metabolic half-life compared to ezutromid (Table 1). Importantly, the most potent compound **50b** showed a slight decrease in half-life compared to ezutromid, and was not affected by the presence of ANF (Table 1). This demonstrates that compound **50b** not only completely retains ezutromid's activity against AhR, but also avoids its metabolic transformation by CYP enzymes that are responsible for hampering ezutromid's sustained efficacy.

Drug	$T_{1/2}$ (min)	$CL_{int(mic)}$ (µL/min/mg)	CL_{int}(liver) (mL/min/kg)
Ezutromid	**60** ± 5	**23.3** ± 2.	**92.4** ± 8.3
Ezutromid + AFN	**89** ± 6	**15.8** ± 1.1	**62.6** ± 4.3
50a	**94** ± 0.2	**14.7** ± 0.1	**58.4** ± 0.4
50a + ANF	**108** ± 11	**12.8** ± 1.4	**50.6** ± 5.4
50b	**40** ± 7	**35.6** ± 7	**140.9** ± 27.9
50b + ANF	**42** ± **4**	**33.6** ± 2.7	**133** ± 10.4
50c	**48** ± **8**	**29.9** ± 4.9	**118.3** ± 19.3
50c + ANF	**56** ± **10**	**25.7** ± 4.6	**102.0** ± 18.1

Table 1: Metabolic stability of new analogues **50a-c**. Stability of new analogues was tested in Mouse Liver Microsomes (MLM) at a concentration of 1µM with or without 3µM ANF, a known inhibitor of CYPs enzymes. **a.** CL_{int}: intrinsic clearance in MLM. CL_{int}(liver) is calculated from Clint and represents an estimation of CL_{int} in mouse liver. **b**. NCF: *no cofactor,* represents the % of remaining drug after 60 minutes incubation without NADPH, indicating the extent of NADPH-dependent metabolism.

CONCLUSIONS

Current bioisosteric replacements for naphthyl rings lack generality and suffer from poor physicochemical properties. We report the first preparation of a diverse series of easily derivatisable sp^3-rich aryl fused BCHeps, serving as bioisosteres for a range of bicyclic (hetero)aromatics, including naphthalene, (iso)quinoline and quinazoline, and the underrepresented β-napthyl unit. The ring frameworks were efficiently accessed *via* an intramolecular crossed [2+2] photocycloaddition through visible light-induced energy transfer, and can be readily transformed into a library of bicyclic isostere building blocks with a range of substitution patterns across the framework. We describe the incorporation of the naphthyl isosteres within the AhR antagonist ezutromid, which suffers from high susceptibility to CYP1A mediated metabolism arising from a naphthyl ring.

With the aid of solid-state structures, cellular assays and metabolic stability studies in mouse liver microsomes, we demonstrate that the aryl-fused BCHep derivatives exhibit geometrically similar substituent vectors to the parent compound, retain biological activity, and display increased metabolic stability relative to their naphthyl counterpart. To the best of our knowledge, this represents the first example of the successful incorporation of a BCHep isostere in a potential pharmaceutical candidate, whilst simultaneously improving the pharmacokinetic properties. This study validates the BCHep motif as a 'true' bioisostere for meta-substituted arenes and naphthalenes.

AUTHOR INFORMATION

Corresponding Author

Angela Russell, Chemistry Research Laboratory, University of Oxford, Mansfield Road, Oxford, OX1 3TA. Email: Angela.russell@chem.ox.ac.uk

ACKNOWLEDGMENT

We gratefully acknowledge the EPSRC for a Strategic Equipment Grant (EP/V028995/1), the MRC for a Development Pathway Funding Scheme award (MR/X014118/1) [AK, LM, SS], and UKRI for a Postdoc Guarantee Fellowship (EP/X028178/1) [MR]. We gratefully acknowledge the EPSRC for a Strategic Equipment Grant (EP/V028995/1) [KC]. We would like to also acknowledge Professor Edward Anderson and Dr Elliot P. Bailey for helpful discussions.

REFERENCES

1. Makar, S., Saha, T. & Singh, S. K. Naphthalene, a versatile platform in medicinal chemistry: Sky-high perspective. *Eur. J. Med. Chem.* **161**, 252-276 (2019).

2. Davies, K. et al. Daily treatment with SMTC1100, a novel small molecule utrophin upregulator, dramatically reduces the dystrophic symptoms in the mdx mouse. *PLoS One.* **6**, 1-10 (2011)

3. Saeed, A. et al. Design, synthesis, biochemical and in silico characterization of novel naphthalene-thiourea conjugates as potential and selective inhibitors of alkaline phosphatase. *Med. Chem. Res.* **32**, 1077-1086 (2023).

4. Jerina, D. et al. The role of arene oxide-oxepin systems in the metabolism of aromatic substrates. III. Formation of 1,2-naphthalene oxide from naphthalene by liver microsomes. *J. Am. Chem. Soc.* **90**, 6525-6527 (1968).

5. Buonarati, M., Morin, D., Plopper, C. & Buckpitt, A. Glutathione depletion and cytotoxicity by naphthalene 1,2-oxide in isolated hepatocytes. *Chem.-Biol. Interact.* **71,** 147-165 (1989).

6. Jerina, D. et. Al. 1,2-Naphthalene oxide as an intermediate in the microsomal hydroxylation of naphthalene. *V. Biochem*. **9**, 147-156 (1970).

7. Taehyeon, M. C., Randy, L. R. & Ernest, H. In vitro metabolism of naphthalene by human liver microsomal cytochrome P450 enzymes. *Drug Metab. Dispos.* **34**, 176-183 (2006).

8. Hu, L., Paul Fawcett, J. & Gu, J. Protein target discovery of drug and its reactive intermediate metabolite by using proteomic strategy. *Acta Pharm. Sin. B.* **2**, 126-136 (2012).

9. Risch, P., Pfeifer, T., Segrestaa, J., Fretz, H. & Pothier, J. Verification of the Major Metabolic Oxidation Path for the Naphthoyl Group in Chemoattractant Receptor-Homologous Molecule Expressed on Th2 Cells (CRTh2) Antagonist 2-(2-(1-Naphthoyl)-8-fluoro-3,4-dihydro-1H-pyrido[4,3-b]indol-5(2H)-yl)acetic Acid (Setipiprant/ACT-129968). *J. Med. Chem.* **58**, 8011-8035 (2015).

10. Chatzopoulou, M. et al. Isolation, Structural Identification, Synthesis, and Pharmacological Profiling of 1,2-trans-Dihydro-1,2-diol Metabolites of the Utrophin Modulator Ezutromid. *J. Med. Chem.* **63**, 2547-2556 (2020).

11. Alison, E. M. V. et al. Multiple Cytochrome P-450s Involved in the Metabolism of Terbinafine Suggest a Limited Potential for Drug-Drug Interactions. *Drug Metab. Dispos.* **27**, 1029-1038 (1999).

12. Buskes, M. J. & Blanco, M. J. Impact of Cross-Coupling Reactions in Drug Discovery and Development. *Molecules* **25** (2020).

13. Chandrasena, G. et al. Identification and optimization of a novel series of [2.2.1]-oxabicyclo imide-based androgen receptor antagonists. *Bioorg. Med. Chem. Lett.* **18**, 1910-1915 (2008).

14. Hadida, S. et al. Discovery of N-(2,4-Di-tert-butyl-5-hydroxyphenyl)-4-oxo-1,4-dihydroquinoline-3-carboxamide (VX-770, Ivacaftor), a Potent and Orally Bioavailable CFTR Potentiator. *J. Med. Chem.* **57**, 9776-9795 (2014).

15. Babbs, A. et al. 2-Arylbenzo[d]oxazole Phosphinate Esters as Second-Generation Modulators of Utrophin for the Treatment of Duchenne Muscular Dystrophy. *J. Med. Chem.* **63**, 7880-7891 (2020).

16. Richardson, B. G. et al. Replacement of a Naphthalene Scaffold in Kelch-like ECH-Associated Protein 1 (KEAP1)/Nuclear Factor (Erythroid-derived 2)-like 2 (NRF2) Inhibitors. *J. Med. Chem.* **61**, 8029-8047 (2018).

17. Wang, Q. et al. Structural basis of the ligand binding and signaling mechanism of melatonin receptors. *Nat. Commun.* **13**, 454 (2022).

18. Chackal-Catoen, S. et al. Dicationic DNA-targeted antiprotozoal agents: Naphthalene replacement of benzimidazole. *Bioorg. Med. Chem.* **14**, 7434-7445 (2006).

19. Nussbaumer, P., Petranyi, G. & Stuetz, A. Synthesis and structure-activity relationships of benzo[b]thienylallylamine antimycotics. *J. Med. Chem.* **34**, 65-73 (1991).

20. Shirinzadeh, H. et al. Bioisosteric modification on melatonin: synthesis of new naphthalene derivatives, *in vitro* antioxidant activity and cytotoxicity studies. *Braz. J. Pharm. Sci.* **56** 1-11 (2020).

21. Rombouts, F. J. R., Tovar, F., Austin, N., Tresadern, G. & Trabanco, A. A. Benzazaborinines as Novel Bioisosteric Replacements of Naphthalene: Propranolol as an Example. *J. Med. Chem.* **58**, 9287-9295 (2015).

22. Sutherland, H. S. et al. Structure-activity relationships for analogs of the tuberculosis drug bedaquiline with the naphthalene unit replaced by bicyclic heterocycles. *Bioorg. Med. Chem.* **26**, 1797-1809 (2018).

23. Bissantz, C., Kuhn, B. & Stahl, M. A medicinal chemist's guide to molecular interactions. *J. Med. Chem.* **53**, 5061-5084 (2010).

24. Wei, W., Cherukupalli, S., Jing, L., Liu, X. & Zhan, P. Fsp^3: A new parameter for drug-likeness. Drug Discov Today **25**, 1839-1845 (2020).

25. Subbaiah, M. A. M. & Meanwell, N. A. Bioisosteres of the Phenyl Ring: Recent Strategic Applications in Lead Optimization and Drug Design. *J. Med. Chem.* **64**, 14046-14128 (2021).

26. Zhang, X. et al. Copper-mediated synthesis of drug-like bicyclopentanes. *Nature* 580, 220-226 (2020).

27. Stepan, A. F. et al. Application of the Bicyclo[1.1.1]pentane Motif as a Nonclassical Phenyl Ring Bioisostere in the Design of a Potent and Orally Active γ-Secretase Inhibitor. *J. Med. Chem.* **55**, 3414-3424 (2012)

28. Frank, N. et al. Synthesis of meta-substituted arene bioisosteres from [3.1.1]propellane. Nature 611, 721-726 (2022).

29. Zhao, J. et al. Intramolecular Crossed [2+2] Photocycloaddition through Visible Light-Induced Energy Transfer. *J. Am. Chem. Soc.* **139**, 9807-9810 (2017).

30. Girvin, Z. C. et al. Asymmetric Photochemical [2 + 2]-Cycloaddition of Acyclic Vinylpyridines through Ternary Complex Formation and an Uncontrolled Sensitization Mechanism. *J. Am. Chem. Soc.* **144**, 20109-20117 (2022).

31. Glorius, F, Strieth-Kalthoff, F. Triplet Energy Transfer Photocatalysis: Unlocking the next Level. *Chem* **6,** 1888-1903 (2020).

32. Xu, W., Wang, W., Liu, T., Xie, J. & Zhu, C. Late-stage trifluoromethylthiolation of benzylic C-H bonds. *Nat. Commun.* **10**, 4867 (2019).

33. Chung, K. Occurrence, uses and carcinogenicity of arylamines. *Front Biosci.* **7**, 322-345 (2015).

34. Glorius, F. et al. Catalytic Access to Alkyl Bromides, Chlorides and Iodides via Visible Light-Promoted Decarboxylative Halogenation. *Chem. Eur, J.* **22**, 9971-9974

35. Cheng, W.-M., Shang, R., Fu, M.-C. & Fu, Y. Photoredox-Catalysed Decarboxylative Alkylation of N-Heteroarenes with N-(Acyloxy)phthalimides. *Chem. Eur. J.,* **23**, 2537-2541 (2017).

36. Khatun, S., Singh, A., Bader, G. N. & Sofi, F. A. Imidazopyridine, a promising scaffold with potential medicinal applications and structural activity relationship (SAR): recent advances. *J Biomol Struct Dyn.* **40**, 14279-14302 (2022).

37. Chancellor, D. R. et al. Discovery of 2-Arylbenzoxazoles as Upregulators of Utrophin Production for the Treatment of Duchenne Muscular Dystrophy. *J. Med. Chem.* **54**, 3241-3250 (2011).

38. Guiraud, S., Roblin, D. & Kay, D. E. The potential of utrophin modulators for the treatment of Duchenne muscular dystrophy. *Expert Opin. Orphan Drugs* **6**, 179-192 (2018).

39. Wilkinson, I. V. L. et al. Chemical Proteomics and Phenotypic Profiling Identifies the Aryl Hydrocarbon Receptor as a Molecular Target of the Utrophin Modulator

Ezutromid. *Angew. Chem. Int. Ed.* **59**, 2420-2428 (2020).

40. Lu, A. et al. Chemical inhibitors of cytochrome P450 isoforms in human liver microsomes: a re-evaluation of P450 isoform selectivity. *Eur. J. Drug Metab. Pharmacokinet.*, **36**, 1-16 (2011).